ACS Photonics

Letter

pubs.acs.org/journal/apchd5

Lasing in a Slow Plasmon Moiré Cavity

Ertugrul Karademir,[†,§] Sinan Balci,[‡] Coskun Kocabas,[†] and Atilla Aydinli*[,†]

[†]Department of Physics, Bilkent University, 06800 Ankara, Turkey

[‡]Department of Astronautical Engineering, University of Turkish Aeronautical Association, 06790 Ankara, Turkey

Supporting Information

ABSTRACT: We report on lasing from dye-based excitons coupled to slow plasmon states inside metallic Moiré cavities. Surface plasmon polaritons (SPPs) inside the cavity were slowed down to a maximum group velocity of 0.3*c*. Varying the modulation of the Moiré cavity, we tune the output wavelength of the plasmonic laser by varying the fast modulation period of the Moiré cavity. This work opens a new way to study SPP−matter interaction dynamics and plasmonic lasing with Bragg cavity confined slow plasmons.

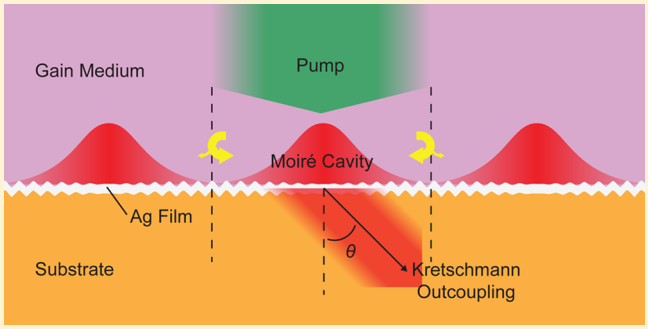

KEYWORDS: *plasmonic laser, strong coupling, slow light, Moiré cavity*

Taming the speed of light opens up new physics for many aspects of light−matter interaction. Increasing the interaction time by slowing down light provides an additional degree of freedom to reduce device size and operating power.[1,2] Slow light has been obtained using quantum interference effects[3,4] as well as photonic crystals[1] and fibers.[5] Work on stimulated Brillouin[5] and Raman[6] scattering making use of the rapid variation of index in the vicinity of Brillouin or Raman gain has also led to slow light. Optical buffers and delays envisioned using slow light, however, suffer from scaling effects due to the wavelength of light.[2] Further confinement of light is possible via the use of surface plasmon polaritons (SPP) using metallic Moiré cavities.[7] In this Letter, we show lasing due to the slow plasmon mode of a metallic Moiré cavity.[8]

Simple plasmonic grating structures interacting with a nearby emitter have been studied for enhancing photoemission,[9−13] owing to the standing wave modes at the band edges. Classical plasmonic Bragg cavity structures[14] have been shown to be useful for investigation of various planar SPP physics.[15] Sophisticated grating structures such as dielectric-loaded biharmonic[11] and Moiré cavities[8,16] are a new class of plasmonic gratings that accommodate a slow propagating cavity mode inside the band gap.[17] We show that such Moiré cavities with slow plasmon modes amplify SPP signal beyond spontaneous emission[18] and exhibit plasmonic lasing action.[12,19−26] Moiré cavities are structurally similar to Bragg cavities that have been in use with DFB lasers[27,28] for reducing spatial hole burning and side mode suppression.[29−32] Here, the cavity mode is confined between amplitude-modulated Bragg mirrors[14] and displays Bragg cavity mode characteristics.[16] Compared to DFB lasers a plasmonic Moiré cavity laser has (i) a smaller confined mode volume and (ii) uses a metallic element for lasing.

Lasing action in plasmonic cavities requires three major components to amplify the signal: a material gain medium interacting with surface plasmons, which helps to compensate for signal loss in the system; a feedback mechanism provided by the metallic grating at the cavity state, where some of the signal is fed back into the gain medium to be further amplified; and a pump source, to excite the gain medium. In a Moiré cavity, the slow plasmon mode is expected to further hasten the lasing action due to increased interaction time between the surface plasmon polariton and the excitonic matter. Population inversion is manifested as a threshold in the pump vs output light signal diagram and is accompanied by a spectral narrowing at the emission wavelength. In addition to the formation of threshold and spectral narrowing, signatures of lasing specific to SPP amplification are related to the plasmon polaritonic nature of the interaction, as indicated by a high TM/TE contrast in the output signal. The polaritonic effect can also be tested through the replacement of the metallic film. Field enhancements due to the surface plasmon modes are sensitive to the optical properties of the metal film used; hence, replacing the metal film dramatically alters the enhancement and lasing properties of the structure. Due to the evanescent nature of the SPP modes, gain medium is located just above the metallic surface where the feedback occurs. This helps to suppress contributions from the optical modes.[33] The emission enhancement due to plasmonic modes at this proximity is comparably larger than the free space emission,[34,35] due to the increased decay rates of the fluorophores involved.[35] SPP amplification in a slow plasmon Moiré cavity provides a further degree of freedom for

Received: April 1, 2015
Published: June 25, 2015

DOI: 10.1021/acsphotonics.5b00168
ACS Photonics 2015, 2, 805−809

future studies on controlled plasmon−matter interaction dynamics.

The experiment setup consists of a Moiré cavity in contact with a laser dye solution (Figure 1a). A Moiré cavity is formed by superposition of two uniform gratings with a sine function profile having 250 and 256 nm pitches (Figure 1b) (see Supporting Information), hereafter referred to as Moiré 250 + 256 nm. The Moiré cavity has fast modulation amplitude with a period of 253 nm and a slowly varying envelope whose period is 10.7 μm. Cavity states are localized at the node of the Moiré cavity where the amplitude of the fast modulation reaches its minimum. SPP characteristics of the Moiré cavity can be understood by constructing polarization-dependent spectroscopic reflection maps. These maps are obtained by recording the reflection spectrum of the sample in Kretschmann configuration at various incidence angles (see Supporting Information). A simulated reflection map is shown in Figure 1c, which is calculated with the finite difference time domain (FDTD) method. The forbidden region in the dispersion relation of the SPPs formed by lifting the degeneracy of the forward and the backward propagating SPP modes[13] gives way to a new state in the Moiré cavity[8] due to the amplitude modulation of the Moiré cavity. The cavity state lies between the two band edges, where the lower band edge with higher frequency is at ∼525 nm and the upper band edge with lower frequency is at ∼550 nm. The same structure in contact with the dye solution (Figure 1d) has similar SPP features with a 170 nm shift to the red of the spectrum. Figure 1e shows the group velocity (v_g) values along the cavity state shown in Figure 1d. The v_g has a maximum at the center of the cavity of 0.16c, where c is the speed of light, and at the edges of the cavity state, it approaches zero. Figure 1f,g show the electric field profiles of the cavity mode marked in Figure 1c,d, respectively. The cavity mode in Figure 1g moves slightly toward the dielectric medium above the cavity structure due to the increase in the effective index. Both modes are localized around the node of the Moiré cavity. (For additional simulation results see Supporting Figures 8 and 9.)

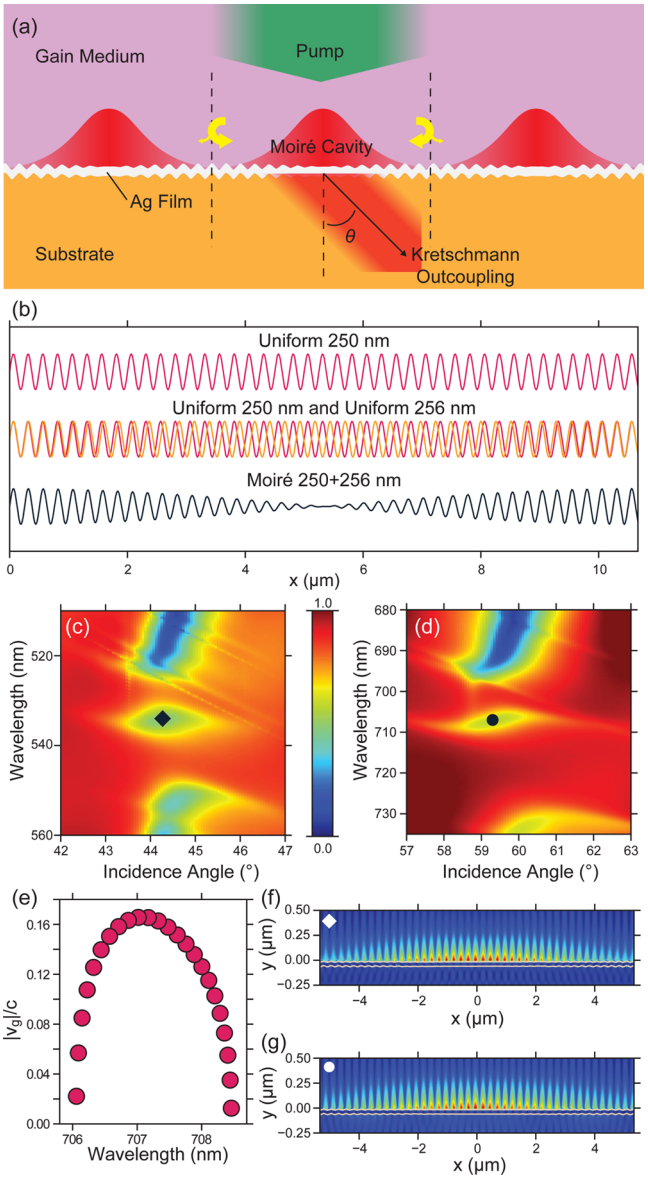

Figure 1. Slowing down SPPs. (a) Schematic description of the amplification process. The SPP cavity mode is excited with near-field coupling. (b) Formation of a Moiré cavity. (c and d) Simulated reflection maps. A cavity mode is created inside the band gap. (c) Reflection map for a Moiré cavity in contact with a vacuum. (d) The same Moiré cavity in contact with the gain medium. (e) Group velocity scaled with the speed of light in a vacuum, along the cavity state. Therefore, the group velocity never exceeds one-fifth of the speed of light inside the cavity. (f and g) Electric field profile of the cavity state at the points marked on the reflection maps in (c) and (d), respectively.

AFM profile of a Moiré 242 + 248 nm before Ag evaporation and a SEM micrograph of the cavity after Ag evaporation are shown in Figure 2a. The cavity is obtained by exposing a

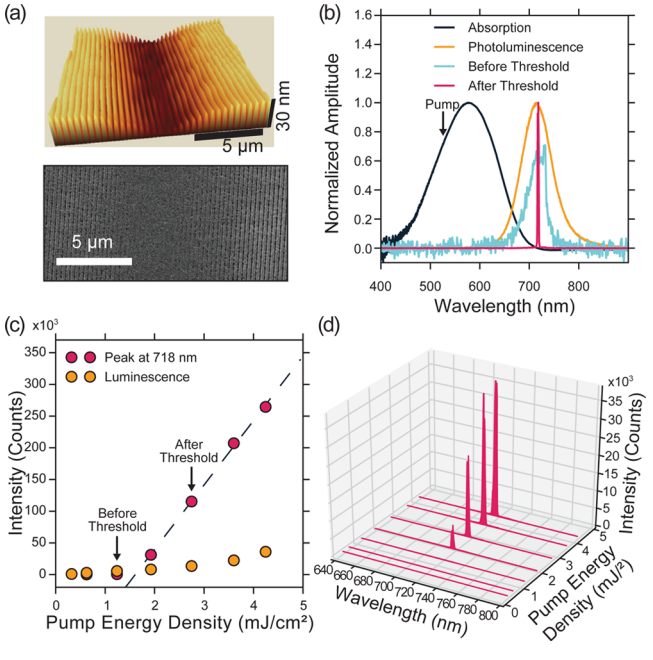

Figure 2. Demonstration of plasmonic lasing. (a) AFM profile before Ag evaporation and SEM micrograph after Ag evaporation of a Moiré cavity with 250 + 256 nm pitch. (b) Absorption and photoluminescence of the gain medium, LDS750 solution, together with the lasing spectrum on the 250 + 256 nm Moiré cavity before and after the lasing threshold. The lasing spectrum has a dramatic spectral narrowing. (c) Intensity of the peak at 718 nm for various pump energy densities. (d) Spectrum at various pump energy densities.

DOI: 10.1021/acsphotonics.5b00168
ACS Photonics 2015, 2, 805−809

photoresist (PR) ($n \simeq 1.56$)-coated soda lime substrate ($n \simeq 1.48$) under a laser interference lithography setup (see Supporting Information). Two sequential exposures are made with different incidence angles to generate large Moiré pattern. The PR pattern is then coated with a 45 nm Ag film by thermal evaporation to support SPPs. As a gain medium, we use Styryl 7, an organic laser dye that is commercially available from Exciton (commercial name LDS750). Styryl 7 is dissolved in extrapure ethylene glycol ($n \simeq 1.4$) solvent from J. T. Baker as a 10 mM batch and then diluted to 5, 2.5, and 0.65 mM solutions (see Supporting Figure 10). Afterward, diluted solutions are injected into a microfluidic channel constructed using two-sided adhesive tapes and soda lime cover glass (see Supporting Figure 6). A pulsed Nd:YAG laser with a BBO crystal is used as 532 nm pump light. The average output power of the pump source is attenuated down to 25.10 mW. The variation of the pump light intensity, from 0.23 to 8.80 mJ/cm^2, is achieved with a series of neutral density filters and polarized filters (see Supporting Figure 3). Neither the incidence angle nor the size of the liquid chamber changes the spectral output of the experiments. Surface plasmon coupled emission (SPCE) is demonstrated in planar metal films[18] and gratings[36] on similar setups. We observed the expected SPCE on planar metal films, uniform gratings, and Moiré cavities (see Supporting Figure 14) at low power densities and are able to obtain lasing with samples that have slow light modes when pump power density exceeds a threshold value. In Figure 2b, we show absorption and luminescence characteristics of the gain medium. Photoluminescence (PL) of the dye under 532 nm illumination shows a broad peak centered around 715 nm having a 60 nm fwhm (145 meV). Under lasing conditions, this peak becomes centered at 718 nm with a fwhm of 2.7 nm (6.5 meV). A comparison between the emission spectrum before and after the lasing threshold indicates a dramatic spectral narrowing. The intensity vs pump energy density plots are obtained by integrating the total area under the lasing peaks, integrating the rest of the luminescence curves, and then plotting them as a function of pump energy density. Above the threshold, the integrated area of the lasing peak is much larger than the integrated area of the rest of the luminescence spectrum. Figure 2c shows the intensity vs pump energy density curve measurements for a Moiré 250 + 256 nm cavity. The threshold energy density is around 1.5 mJ/cm^2. Below the threshold value, both integrations give approximately the same results; beyond the 1.5 mJ/cm^2 mark, there is a linear increase in the lasing peak intensity.

Figure 3a,b show the experimentally obtained reflection maps for the Moiré 250 + 256 nm cavity in the air and in the dye solution, respectively. The 1 marks the cavity state that is supporting the lasing action, whereas 2 and 3 mark the upper and the lower plasmonic band edges, respectively. In Figure 3b, modes marked with 4 are SPP modes on the opposite sides of the metallic film, in this case the metal−PR interface (Supporting Figure 9). Considering both sides of the metallic grating, there are two modes: one is created along the metal−upper dielectric interface, and the other at the metal−lower dielectric interface. Modes on the opposite side can be excited via the grating structure.[9,10,37] These modes are isolated from the interaction on the upper face of the metal film. The spectral position of the cavity state in Figure 3a is around 545 nm in air, and because the sample is in the dye solution, all of the SPP modes are shifted to the red of the electromagnetic spectrum in Figure 3b. Figure 3e,f show the group velocity for the cavity

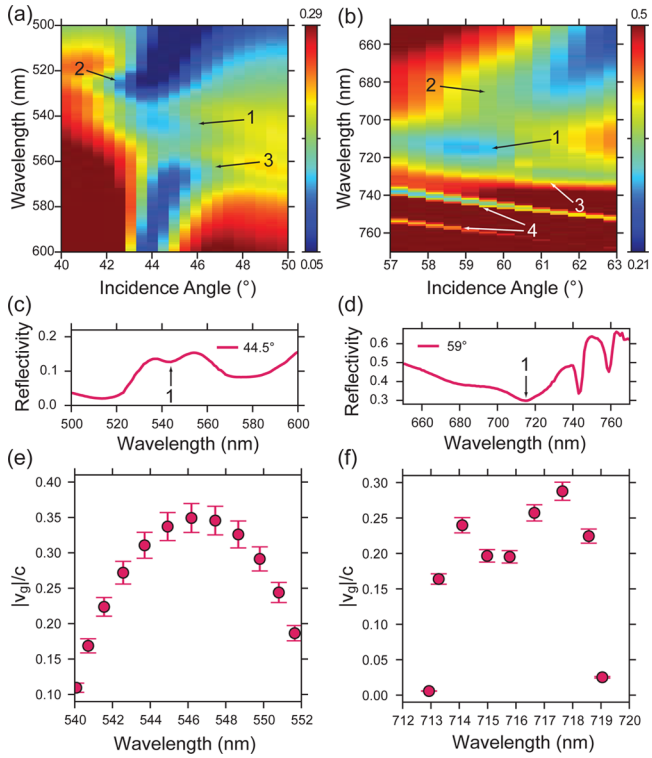

Figure 3. Role of the Moiré cavity in plasmonic lasing. (a) Reflection map of Moiré 250 + 256 nm in air. Feature 1 is the cavity mode, 2 is the upper band edge, and 3 is the lower band edge. In LDS 750 dye solution, (b) all plasmonic features (1−3) are shifted toward the red. We observe SPPs at the metal−PR interface marked with 4. (c and d) Reflection data at 44.5° incidence angle in air and 59° incidence angle in solution, respectively. (e and f) Group velocity scaled with the speed of light along the cavity states shown in (a) and (b), respectively. Double peak in (f) is due to an error caused by the modes at the Ag−PR interface.

modes shown in Figure 3a,b, respectively. In both cases v_g does not exceed about 0.35c; in the dye solution v_g is 0.25c at the center of the mode, approaching the calculated value. As expected, v_g approaches zero at the edges of the cavity state. The lasing is observed when v_g starts to decrease in Figure 3f. Reduced speed (~0.3c) at this edge gives way to plasmonic enhancement and amplification, and we observe the lasing peak at around 718 nm wavelength. The quality factor of the plasmonic mode along the cavity is about 4 times larger than that of the band edge (see Supporting Figure 12), which makes the feedback in the cavity mode-dominant over that along the band edge. The experimental results confirm the calculated results. Cavity states are located at the expected k values (1.24 × 10^7 m^{-1}), and the cavity centers are close to the same wavelengths. Small differences can be attributed to oxidation of the Ag film (around 2 nm), imperfect grating profiles, and the experimental errors while extracting optical parameters of the dielectric films (see Supporting Information for detailed experimental methods).

In order to vary the central frequency of the cavity mode, we fabricated three different Moiré cavities, labeled 242 + 248 nm, 250 + 256 nm, and 260 + 266 nm, and compared the plasmonic lasing performance of the Moiré cavities in Figure 4a. The 242 + 248 nm Moiré cavity has its lasing peak at 713 nm with a fwhm of 1.34 nm (3.3 meV), and the 250 + 256 nm Moiré cavity has its lasing peak at 718 nm with a fwhm of 2.7 nm (6.5

DOI: 10.1021/acsphotonics.5b00168
ACS Photonics 2015, 2, 805−809

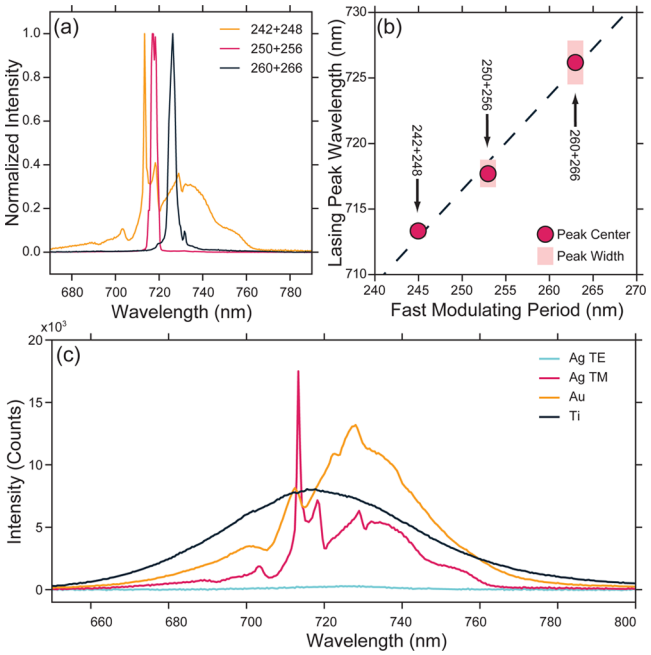

Figure 4. Plasmonic lasing confirmation tests. (a) Comparison of plasmonic lasing for various Moiré cavities. (b) Proportional shift due to the cavity shape change shown in detail. For all three samples, cavity size is around 10 μm; hence the fast modulating period determines the peak wavelength of the cavity state. (c) Comparison of spectra of the Moiré cavity (242 + 248 nm) with different material coatings and light polarizations. We observe the lasing peak only in the Ag-coated sample, and the output is highly TM polarized.

meV), while the 260 + 266 nm Moiré cavity has its lasing peak at 726 nm with a fwhm of 2.8 nm (6.5 meV). As the cavity states of these gratings shift, we observe a proportional shift in the lasing peak wavelength (Figure 4b), which validates that the plasmonic lasing action is indeed due to the cavity modes. We also expect that replacing the material of the metal film should alter the lasing behavior. Au and Ag are well known for their SPP properties in the visible spectrum, whereas Ti does not support SPP modes in this part of the spectrum. Figure 4c shows PL spectra obtained with the 242 + 248 nm Moiré cavities coated with different metals. Au-coated samples exhibit SPP features, but no lasing peak is observed. In the visible part of the spectrum, it is well known that Au has a lower SPP resonance frequency compared to Ag, and the SPPs on Ag have longer lifetimes compared to the SPPs on Au.[38] We suspect that the shorter plasmonic lifetime of Au and the quality of Au films might be responsible for the lack of lasing. Ti-coated samples exhibit only a PL spectrum of the dye solution. Ag-coated samples, on the other hand, exhibit lasing peaks, and these peaks are highly TM polarized (see Supporting Figure 5), which is another fingerprint of SPP-based amplification. Since SPP modes are excited with the near-field coupling, on rotating the polarization of the source to the TE direction and probing the output for TM/TE contrast, we observe (see Supporting Figure 5) the same TM/TE distinction (no SPP features in TE, SPP features in TM) at the output under both TE and TM excitation.

In conclusion, we demonstrated lasing based on the slow plasmon modes of Moiré cavity structures. This flexible plasmonic platform allows us to control the group velocity of SPPs and greatly amplifies the emission of the organic dyes, quantum dots, and other excitonic systems such as J-aggregates. Here lasing action in Moiré cavities is enabled by slow SPPs at the edges of the cavity modes, where the group velocity tends toward zero. Furthermore, lasing wavelength is tunable since the periodicity of the Moiré cavity determines the resonance frequency of the cavity mode. This demonstration, to our knowledge, is the first one that shows that the slow plasmonic modes of a grating cavity structure interacting with an exciton medium can amplify the SPP signal. Lasing efficiency can be further improved by reducing the scattering losses using an epitaxially grown metallic film instead of a thermally evaporated metal film. This would also reduce the ohmic losses of SPP modes and should bring the lasing threshold energy further down and increase the light output. Future work may include plasmonic amplification in different parts of the spectrum. This work opens the way to study the interaction dynamics of slow plasmons with excitons.

■ ASSOCIATED CONTENT

Supporting Information

Detailed information on Moiré gratings and additional data related to lasing as well as a detailed explanation of the experimental methods. The Supporting Information is available free of charge on the ACS Publications website at DOI: 10.1021/acsphotonics.5b00168.

■ AUTHOR INFORMATION

Corresponding Author

*E-mail: aydinli@fen.bilkent.edu.tr.

Present Address

[§]School of Physics and CRANN, Trinity College Dublin, Dublin 2, Ireland.

Notes

The authors declare no competing financial interest.

■ ACKNOWLEDGMENTS

This work is supported by the Research Council of Turkey, TUBITAK, via grants 110T790, 110T589, and 112T091. E.K. acknowledges Askin Kocabas for his valuable input during discussion of the results.

■ REFERENCES

(1) Goban, A.; Hung, C.-L.; Yu, S.-P.; Hood, J. D.; Muniz, J. A.; Lee, J. H.; Martin, M. J.; McClung, A. C.; Choi, K. S.; Chang, D. E.; Painter, O.; Kimble, H. J. Atom–light Interactions in Photonic Crystals. *Nat. Commun.* **2014**, *5*, 4808.

(2) Mookherjea, S.; Park, J. S.; Yang, S.-H.; Bandaru, P. R. Localization in Silicon Nanophotonic Slow-Light Waveguides. *Nat. Photonics* **2008**, *2*, 90–93.

(3) Hau, L. V.; Harris, S. E.; Dutton, Z.; Behroozi, C. H. Light Speed Reduction to 17 Metres per Second in an Ultracold Atomic Gas. *Nature* **1999**, *397*, 594–598.

(4) Lukin, M. D.; Imamoğlu, A. Controlling Photons Using Electromagnetically Induced Transparency. *Nature* **2001**, *413*, 273–276.

(5) Okawachi, Y.; Bigelow, M. S.; Sharping, J. E.; Zhu, Z.; Schweinsberg, A.; Gauthier, D. J.; Boyd, R. W.; Gaeta, A. L. Tunable All-Optical Delays via Brillouin Slow Light in an Optical Fiber. *Phys. Rev. Lett.* **2005**, *94*, 153902.

(6) Okawachi, Y.; Foster, M.; Sharping, J.; Gaeta, A.; Xu, Q.; Lipson, M. All-Optical Slow-Light on a Photonic Chip. *Opt. Express* **2006**, *14*, 2317–2322.

(7) Sandtke, M.; Kuipers, L. Slow Guided Surface Plasmons at Telecom Frequencies. *Nat. Photonics* **2007**, *1*, 573–576.

DOI: 10.1021/acsphotonics.5b00168
ACS Photonics 2015, 2, 805–809

(8) Kocabas, A.; Senlik, S. S.; Aydinli, A. Slowing Down Surface Plasmons on a Moiré Surface. *Phys. Rev. Lett.* **2009**, *102*, 063901.
(9) Wedge, S.; Hooper, I. R.; Sage, I.; Barnes, W. L. Light Emission through a Corrugated Metal Film: The Role of Cross-Coupled Surfaceplasmon Polaritons. *Phys. Rev. B: Condens. Matter Mater. Phys.* **2004**, *69*, 245418.
(10) Gruhlke, R. W.; Holland, W. R.; Hall, D. G. Surface Plasmon Cross Coupling in Molecular Fluorescence near a Corrugated Thin Metal Film. *Phys. Rev. Lett.* **1986**, *56*, 2838−2841.
(11) Kocabas, A.; Ertas, G.; Senlik, S. S.; Aydinli, A. Plasmonic Band Gap Structures for Surface-Enhanced Raman Scattering. *Opt. Express* **2008**, *16*, 12469−12477.
(12) Okamoto, T.; H'Dhili, F.; Kawata, S. Towards Plasmonic Band Gap Laser. *Appl. Phys. Lett.* **2004**, *85*, 3968−3970.
(13) Kitamura, Y.; Murakami, S. Hermitian Two-Band Model for One-Dimensional Plasmonic Crystals. *Phys. Rev. B: Condens. Matter Mater. Phys.* **2013**, *88*, 045406.
(14) Weeber, J.-C.; Bouhelier, A.; Colas des Francs, G.; Markey, L.; Dereux, A. Submicrometer In-Plane Integrated Surface Plasmon Cavities. *Nano Lett.* **2007**, *7*, 1352−1359.
(15) Derom, S.; Bouhelier, A.; Kumar, A.; Leray, A.; Weeber, J.-C.; Buil, S.; Quélin, X.; Hermier, J. P.; Francs, G. C. des. Single-Molecule Controlled Emission in Planar Plasmonic Cavities. *Phys. Rev. B: Condens. Matter Mater. Phys.* **2014**, *89*, 035401.
(16) Balci, S.; Karabiyik, M.; Kocabas, A.; Kocabas, C.; Aydinli, A. Coupled Plasmonic Cavities on Moire Surfaces. *Plasmonics* **2010**, *5*, 429−436.
(17) Balci, S.; Karademir, E.; Kocabas, C.; Aydinli, A. Direct Imaging of Localized Surface Plasmon Polaritons. *Opt. Lett.* **2011**, *36*, 3401−3403.
(18) Chen, Y.-H.; Li, J.; Ren, M.-L.; Li, Z.-Y. Amplified Spontaneous Emission of Surface Plasmon Polaritons with Unusual Angle-Dependent Response. *Small* **2012**, *8*, 1355−1359.
(19) Bergman, D. J.; Stockman, M. I. Surface Plasmon Amplification by Stimulated Emission of Radiation: Quantum Generation of Coherent Surface Plasmons in Nanosystems. *Phys. Rev. Lett.* **2003**, *90*, 027402.
(20) Seidel, J.; Grafström, S.; Eng, L. Stimulated Emission of Surface Plasmons at the Interface between a Silver Film and an Optically Pumped Dye Solution. *Phys. Rev. Lett.* **2005**, *94*, 177401.
(21) Oulton, R. F.; Sorger, V. J.; Zentgraf, T.; Ma, R.-M.; Gladden, C.; Dai, L.; Bartal, G.; Zhang, X. Plasmon Lasers at Deep Subwavelength Scale. *Nature* **2009**, *461*, 629−632.
(22) Noginov, M. A.; Zhu, G.; Belgrave, A. M.; Bakker, R.; Shalaev, V. M.; Narimanov, E. E.; Stout, S.; Herz, E.; Suteewong, T.; Wiesner, U. Demonstration of a Spaser-Based Nanolaser. *Nature* **2009**, *460*, 1110−1112.
(23) Zheludev, N. I.; Prosvirnin, S. L.; Papasimakis, N.; Fedotov, V. A. Lasing Spaser. *Nat. Photonics* **2008**, *2*, 351−354.
(24) Zhou, W.; Dridi, M.; Suh, J. Y.; Kim, C. H.; Co, D. T.; Wasielewski, M. R.; Schatz, G. C.; Odom, T. W. Lasing Action in Strongly Coupled Plasmonic Nanocavity Arrays. *Nat. Nanotechnol.* **2013**, *8*, 506−511.
(25) Schokker, A. H.; Koenderink, A. F. Lasing at the Band Edges of Plasmonic Lattices. *Phys. Rev. B: Condens. Matter Mater. Phys.* **2014**, *90*, 155452.
(26) Yang, A.; Hoang, T. B.; Dridi, M.; Deeb, C.; Mikkelsen, M. H.; Schatz, G. C.; Odom, T. W. Real-Time Tunable Lasing from Plasmonic Nanocavity Arrays. *Nat. Commun.* **2015**, *6*, 6939.
(27) Kogelnik, H.; Shank, C. V. Stimulated Emission in a Periodic Structure. *Appl. Phys. Lett.* **1971**, *18*, 152−154.
(28) Coldren, L. A. Monolithic Tunable Diode Lasers. *IEEE J. Sel. Top. Quantum Electron.* **2000**, *6*, 988−999.
(29) Morthier, G.; David, K.; Vankwikelberge, P.; Baets, R. A New DFB-Laser Diode with Reduced Spatial Hole Burning. *IEEE Photonics Technol. Lett.* **1990**, *2*, 388−390.
(30) Girardin, F.; Duan, G.-H.; Talneau, A. Modeling and Measurement of Spatial-Hole-Burning Supplied to Amplitude Modulated Coupling Distributed Feedback Lasers. *IEEE J. Quantum Electron.* **1995**, *31*, 834−841.
(31) Talneau, A.; Chandouineau, J. P.; Charil, J.; Ougazzaden, A. Suppression of Fringe Diffraction in Localized Holographic Exposure for DFB Laser Arrays. *IEEE Photonics Technol. Lett.* **1995**, *7*, 721−723.
(32) Talneau, A.; Charil, J.; Ougazzaden, A.; Bouley, J. C. High Power Operation of Phase-Shifted DFB Lasers with Amplitude Modulated Coupling Coefficient. *Electron. Lett.* **1992**, *28*, 1395−1396.
(33) Gather, M. C. A Rocky Road to Plasmonic Lasers. *Nat. Photonics* **2012**, *6*, 708−708.
(34) Carniglia, C. K.; Mandel, L.; Drexhage, K. H. Absorption and Emission of Evanescent Photons. *J. Opt. Soc. Am.* **1972**, *62*, 479−486.
(35) Lakowicz, J. R. Radiative Decay Engineering: Biophysical and Biomedical Applications. *Anal. Biochem.* **2001**, *298*, 1−24.
(36) H'Dhili, F.; Okamoto, T.; Simonen, J.; Kawata, S. Improving the Emission Efficiency of Periodic Plasmonic Structures for Lasing Applications. *Opt. Commun.* **2011**, *284*, 561−566.
(37) Pockrand, I. Coupling of Surface Plasma Oscillations in Thin Periodically Corrugated Silver Films. *Opt. Commun.* **1975**, *13*, 311−313.
(38) Stockman, M. I. Nanoplasmonics: Past, Present, and Glimpse into Future. *Opt. Express* **2011**, *19*, 22029−22106.

DOI: 10.1021/acsphotonics.5b00168
ACS Photonics 2015, 2, 805−809